IEEE Access
Multidisciplinary | Rapid Review | Open Access Journal

Received May 28, 2020, accepted June 8, 2020, date of publication June 12, 2020, date of current version June 24, 2020.

Digital Object Identifier 10.1109/ACCESS.2020.3001976

An Effective Ship Control Strategy for Collision-Free Maneuver Toward a Dock

YONGHUI SHUAI[1,2], GUOYUAN LI[1], (Senior Member, IEEE), JINSHAN XU[2], (Member, IEEE), AND HOUXIANG ZHANG[1], (Senior Member, IEEE)

[1]Department of Ocean Operations and Civil Engineering, Norwegian University of Science and Technology, 6009 Aalesund, Norway
[2]College of Computer Science and Technology, Zhejiang University of Technology, Hangzhou 310023, China

Corresponding author: Guoyuan Li (guoyuan.li@ntnu.no)

This work was supported in part by the Project Digital Twins for Vessel Life Cycle Service, under Grant 280703 from Research Council of Norway, and in part by the Project Dynamic Motion Planning Based on Trajectory Prediction in Close-Range Manoeuvring, under Grant 298399 from Research Council of Norway.

ABSTRACT Ship maneuvering toward a dock is a hot research topic in the field of autonomous ships. How to realize autonomous low-speed maneuver to a designated location under environmental disturbances is the fundamental problem at present. In addition, potential collisions with other nearby vessels and evasive maneuvers that meet maritime regulations increase the complexity of maneuvering. This paper presents an effective ship control strategy for collision-free maneuver toward a dock. In the strategy, a line-of-sight (LOS) algorithm is utilized to steer the ship along a pre-planned path toward the dock. A collision risk factor that takes ship's maneuvering characteristics, ship domain and relative velocity into account is designed for collision avoidance. Evasive maneuvers complying with the main rules of the international collision avoidance regulations at sea can be achieved based on the risk factor. A ship bumper is constructed, based on which the strategy can switch to either ''path following'' or ''collision avoidance''. Numerical simulations for different encounter situations including head-on, starboard-crossing and overtaking under wind perturbations are carried out. The results show the proposed strategy is able to keep the ship domain free during maneuvering and steer the ship to the docking area in a safe and appropriate manner.

INDEX TERMS Ship maneuvering, risk factor, line-of-sight algorithm, collision avoidance, ship domain.

I. INTRODUCTION

With the rapid development of economic globalization, the quantum of international trade continues to increase. Maritime transportation as the main mode of freight transportation accounts for about 70% of the total international trade. Autonomous ships are considered the future of the maritime industry for transportation, as it can realize cost-effective shipping while ensuring ship safety. To achieve the goal, however, there are many practical problems that need to be solved at present. One of the most significant problems is how to steer the autonomous ship to a dock in a safe and efficient manner.

In fact, ship maneuvering in harbor areas under certain environmental conditions is a challenging manoeuvring assignment for captains, since the environmental perturbations, such as wind, wave and current, have a great impact on ship hull. Furthermore, the limited work space, the positioning, and the heading requirements for harbor operations and the marine ships nearby constitute a complex environment. During maneuvering to a dock, the captain needs to know the ship's current state and observe surroundings in order to avoid grounding and collision with obstacles, the dock and other ships nearby. To guarantee effective collision-free operations, the International Regulations for Prevent Collision at Sea (COLREGs) introduced by the International Maritime Organization (IMO) [1] should also be adopted. This regulation guides the captains how to take actions in different encounter situations.

For an autonomous ship, taking advantage of its on-board sensors, it is possible to perceive the environment and thus realize collision-free maneuver in harbor areas. In this paper, we design a line-of-sight (LOS) based ship control strategy incorporated with COLREGs-compliant anti-collision mechanism for autonomous maneuver to a dock. The main contributions of this paper can be summarized as follows:

1) Establish an LOS based controller for ship maneuvering toward a dock.

The associate editor coordinating the review of this manuscript and approving it for publication was Zhe Xiao.

2) Construct ship bumper and propose a concept of collision risk factor that takes maneuverability, ship domain, and relative velocity into account.
3) Design a risk based ship collision avoidance mechanism complying with partial rules of the COLREGs.

The rest of the paper is organized as follow: Section II is a brief overview of related work. In Section III, an LOS based controller together with a ship collision avoidance mechanism is introduced. Section IV presents the maneuvering results of the approach for different encounter situations under wind perturbation. Conclusions and future work are given in Section V.

II. RELATED WORK

It has seen an increasing interest in developing robust control system for ship maneuvering in the last decade. The sliding mode control (SMC) [2], which is one of the most popular nonlinear control methods, has been employed to design automatic maneuvering system. For example, in 2013, Mizuno et al. developed an SMC based ship maneuvering system that is capable of steering a ship to a desired destination [3]. Later, they improved the system by applying optimal preview SMC with an adaptation mechanism [4]. Yuan and Wu proposed a terminal sliding mode fuzzy control method for nonlinear ship autopilot systems. The results show it can eliminate the chattering and make the system more robust [5]. Maki et al. converted the off-line automatic berthing problem into a minimum-time optimization problem, and employed covariance matrix adaption evolution strategy to resolve this problem [6].

Besides SMC, the nonlinear algorithm is another solution to ship maneuvering for docking. It requires higher computational resources to obtain a optimal maneuver path [7]. Nevertheless, taking advantages of graphics processing units, nonlinear algorithm can be executed in parallel, which makes it possible to achieve optimal control in real time [8]. In 2015, Mizuno et al. proposed a quasi real-time optimal auto-berthing control scheme that contains a multiple shooting algorithm for path generation and a model predictive controller for path following under constant wind disturbance [9].

The first automatic ship berthing system based on artificial neural networks (ANN) was investigated in 1990 by Yamato [10]. In 2001, Im and Hasegawa presented a parallel neural network based controller to adjust ship thruster shaft speed and rudder angle [11]. The developed controller could work under slight influences of wind and current, but will fail in harsh environment. Inspired by [11], Similar work has been done by Nguyen and Jung by using adaptive neural networks [12]. Ahmed et al. first tried to use the concept of virtual windows to ensure the consistency of training data, and established automatic ship berthing system based on ANN [13], [14]. Shuai et al. developed an ANN with parallel structure for ship berthing [15]. The ANN-based controller shows good performance even under dynamic wind conditions. There are also researches that directly utilize real ship maneuvering data obtained from successful berths, to train ANN-based controllers [16], [17]. Nevertheless, these methods are not applicable to general docking operation, as it is difficult to collect enough ship berthing data under different environmental conditions for training.

Collision avoidance is of great importance for ships in close-range encounters. Efforts have been made to realize collision-free maneuver for years [18], [19]. For example, Shen et al. proposed a deep reinforcement learning based collision avoidance method for multiple ships in restricted waters [20]. They applied a ship bumper (i.e., the extension of the bow and the stern parts of a ship along the semi-major axis and the semi-minor axis) to assess the risk of collision, based on which they further designed a safe coefficient to switch between ''normal mode'' and ''collision avoidance mode'' for ship navigation. Johansen et al. introduced a model predictive control based collision avoidance system for ships [21]. They designed a cost function involving the predicted trajectories, collision hazards, and compliance with the rules in COLREGs, to optimize collision-free maneuvers. Lee et al. proposed a multi-ship collision avoidance and path generating algorithm based on the velocity potential functions [22]. The ship can achieve the collision evasive maneuver according to the vector field of vortex potential and the track-keeping maneuver in accordance with the vector field of dipole potential.

III. DESIGN OF SHIP CONTROL STRATEGY

The objective of this research is to design an effective ship control strategy to achieve collision-free maneuver for a ship steering toward a dock. This section describes what the problem of ship maneuvering for docking is, and how we design the control strategy to address it.

A. PROBLEM STATEMENT AND PROPOSED SOLUTION

In practice, the docking process can be divided into two phases: a ballistic phase and a side-push phase. In this paper, we focus on the first phase and try to solve the problem of collision-free maneuver of a ship starting at a distance $15\sim18$ times of the ship length away from the docking area. As mentioned in Section I, sailing a ship toward a dock needs to take the environmental effects, the surrounding marine traffic, and the rules of COLREGs into account. Taking the ferries sailing between Hareid-Sulesund in Norway as an example: there are at least 3 shuttle ferry connections in the region. Moreover, there are usually $3\sim5$ large cruise vessels passing the ferry docking facilities on a normal day during summer. The task requires the ferry not only to avoid collision with the ships nearby, but also to decelerate and eventually stop at a desired docking area. Fig. 1 shows such a schematic scenario. Two coordinate systems are used, i.e., the north-up coordinate system $\{o\} = (x_o, y_o)$, and the body coordinate system $\{b\} = (x_b, y_b)$. The symbols appeared in Fig. 1 is illustrated Table 1.

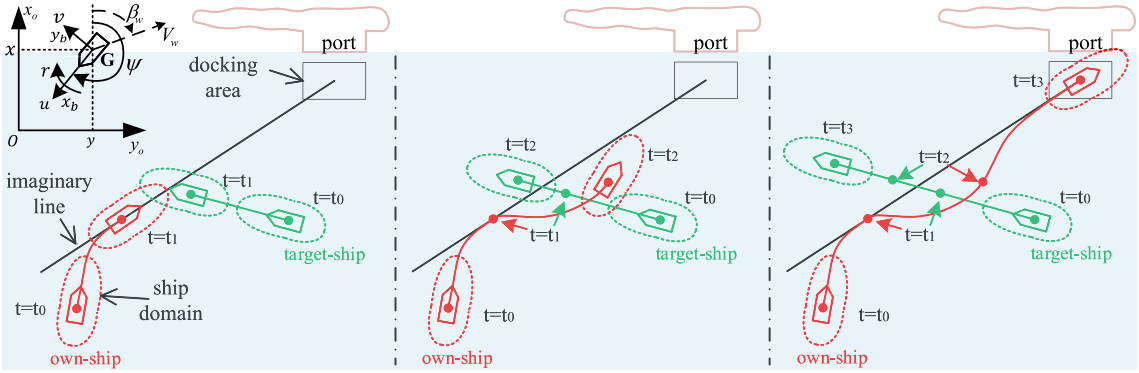

FIGURE 1. Scenario of ship maneuvering to a dock.

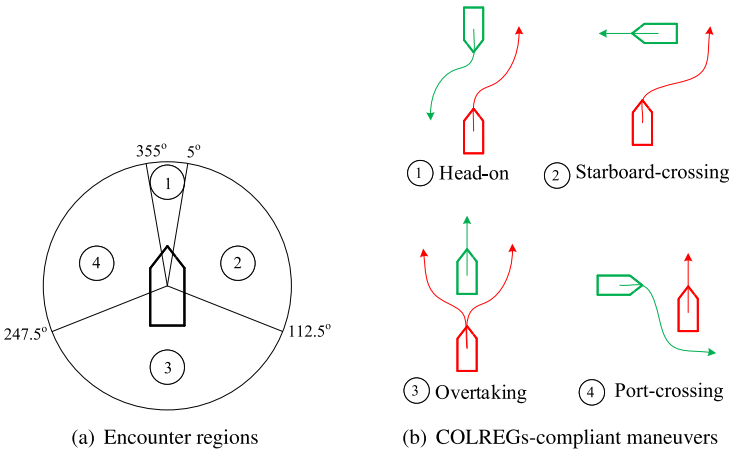

FIGURE 2. The own ship's encounter regions and its maneuvers according to rules 13-15 in COLREGs.

TABLE 1. Notation for ship maneuvering.

Symbol	Description
G	The center of gravity
β_w, V_w	Relative wind direction and speed expressed in $\{o\}$
u, v, r	Surge, sway and yaw velocities expressed in $\{b\}$
x, y, ψ	Position and heading expressed in $\{o\}$

Inspired by [14], we apply the concept of an imaginary line to ensure a safe and appropriate maneuver to the dock. The imaginary line, as shown in Fig. 1, is an empirical path often used by captains to direct their ships toward the dock. In general, the path has an angle about $20^\circ \sim 40^\circ$ to the dock, and its length can be 15 to 18 times of the ship length. The docking maneuver problem can thus be simplified as a path following problem, and be solved using tracking algorithms.

Collision avoidance in close-range encounters is another problem that needs to be solve in this study. To distinguish all encountered ships, here the direct controlled ship is defined as the own ship, whereas other involved ships are considered as the target ships. Two assumptions are made to reduce the difficulty of the task: (1) all ships in encounters are identical power-driven ships, and (2) each ship can observe its status, such as position, heading and velocity, and the status of surrounding ships through the on-board sensor system. Followed the works from [23], [24], the region of the own ship is divided into four encounter regions according to the position of the target ship, as shown in Fig. 2 (a). A ship in an encounter can act to either "give way" or "stand on". We take the main rules in COLREGs (rules 13-15) as reference to create actions for the own ship, as shown in Fig. 2 (b). The own ship has to take give-way actions in head-on, starboard-crossing and overtaking encounters, and keep the speed and the course in port-crossing encounter. This paper mainly focuses on the evasive maneuvers in head-on, starboard-crossing and overtaking encounters.

Based on the assumptions and the main focus of the paper, a ship control strategy for this maneuvering task is proposed, as shown in Fig. 3. The strategy consists of two closed loops: one is used to take actions according to the main rules in

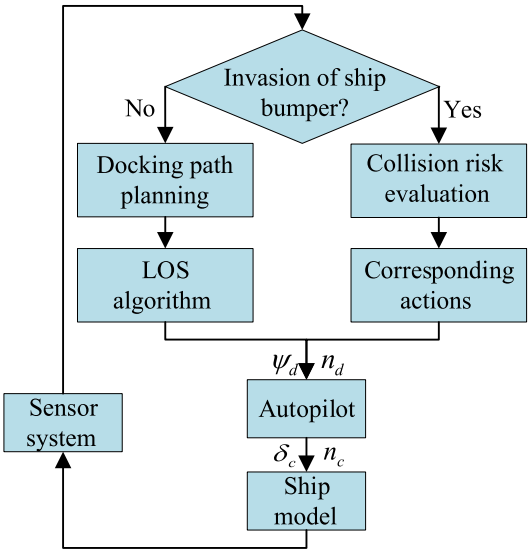

FIGURE 3. Diagram of ship control strategy for maneuvering to a dock.

COLREGs for collision avoidance; the other is responsible for path following toward the dock. The two loops can be switched back and forth, depending on whether the ship bumper of the own ship (see details in Section III-D2) is invaded or not (the condition is equivalent to $f_{risk} > 0$, which will be introduced in Section III-D3). Both loops generate a pair of reference signals, i.e., the desired heading angle ψ_d and the desired thruster shaft speed n_d for autopilot. These signals are further processed to create control commands, i.e., the rudder angle command δ_c and the shaft speed command n_c, for ship motion generation.

B. SHIP MOTION MODELING

Ship motions in a horizontal plane, including surge, sway and yaw, have dynamics resulting from the propulsion system and environmental perturbations. In order to simulate a ship's motion in response to the control commands and environmental effects, the standard three degrees of freedom ship dynamics model that ignores the roll, pitch and heave motions are used [25]:

$$\begin{aligned} \dot{\eta} &= R(\psi)\nu \\ M\dot{\nu} + C(\nu)\nu + D(\nu)\nu &= \tau_c + \tau_w \end{aligned} \tag{1}$$

where $\eta = [x, y, \psi]^\top$ includes ship position and heading in $\{o\}$; $\nu = [u, v, r]^\top$ represents ship velocities in $\{b\}$; $R(\psi)$ stands for rotation matrix; M is the ship inertia matrix; $C(\nu)$ and $D(\nu)$ are Coriolis and damping matrix, respectively; τ_c denotes the commanded forces and moment in $\{o\}$, consisting of the forces and moment from propellers $\tau_P = [X_P, Y_P, N_P]^\top$ and rudders $\tau_R = [X_R, Y_R, N_R]^\top$; $\tau_w = [X_W, Y_W, N_W]^\top$ is the forces and moment in $\{o\}$ caused by wind disturbance.

In this study, a thruster-rudder model is used for steering the ship [26]. As the thruster mainly produces longitudinal force, its hydrodynamic model can be written as:

$$\begin{aligned} X_p &= (1 - t_P)T \\ Y_P &= 0 \\ N_P &= 0 \end{aligned} \tag{2}$$

where t_P is a coefficient; T is the nominal thrust, which is expressed as:

$$T = \rho n^2 D_p^4 k_T \tag{3}$$

where ρ is water density; n is thruster shaft speed (rpm); D_p is diameter of the propeller; and k_T is the thrust coefficient. The hydrodynamic forces and moment generated by the rudder can be calculated by:

$$\begin{aligned} X_R &= -(1 - t_R)F_N \sin\delta \\ Y_R &= -(1 + a_H)F_N \cos\delta \\ N_R &= -(x_R + a_H x_H)F_N \cos\delta \end{aligned} \tag{4}$$

where t_R and a_H are constant coefficients; x_R and x_H are the distances from the rudder and the propeller to the ship's center of gravity, respectively; F_N is the rudder pressure; δ denotes the rudder angle.

The wind disturbance is considered here, as it has a significant effect on ship motion. The wind forces and moment acting on the ship can be estimated as [27]:

$$\begin{aligned} X_W &= \frac{1}{2} C_X \rho_a V_r^2 A_F \\ Y_W &= \frac{1}{2} C_Y \rho_a V_r^2 A_L \\ N_W &= \frac{1}{2} C_N \rho_a V_r^2 A_L L \end{aligned} \tag{5}$$

The corresponding physical meaning of each symbol is listed in Table 2.

TABLE 2. Parameters of wind force model.

Symbol	Physical meaning
ρ_a	Air density
A_F	Frontal projected area of ship
A_L	Lateral projected area of ship
V_r	Relative wind speed
X_W	Fore-aft component of wind force
Y_W	Lateral component of wind force
N_W	Yawing moment
C_X,C_Y,C_N	Coefficients calculated using Isherwood72
L	Ship length

C. PATH FOLLOWING METHOD

As mentioned in Section III-A, it is practical that the ship approaches the dock area with a certain angle, along with an imaginary line. To ensure the ship can follow the pre-planned path, the LOS algorithm with acceptance circle option is applied, as shown in Fig. 4. Suppose the ship position (x, y) and its velocity U are given, the distance error e, i.e., (the normal distance to the planned path) can be calculated. By defining a circle with a radius $R = \alpha e$ $(\alpha > 1)$, we can obtain the

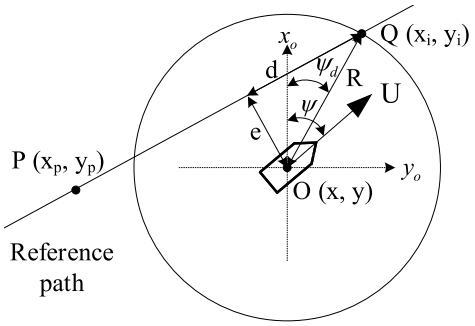

FIGURE 4. Schematic representation of LOS algorithm with acceptance circle option.

position (x_i, y_i) of the intersection point Q between the circle and the path (choose the point closer to the destination) by solving the following equations:

$$\begin{aligned}(x_i - x)^2 + (y_i - y)^2 &= R^2 \\ \frac{x_i - x_p}{y_i - y_p} &= k\end{aligned} \tag{6}$$

where (x_P, y_P) is the position of the way point P on the planned path; k is a constant representing the slope of the planned path. After that, a desired heading angle can thus be obtained:

$$\psi_d = arctan(\frac{x_i - x}{y_i - y}) \tag{7}$$

For thruster shaft speed, it is designed as a piece-wise function to ensure the ship approach the dock in a safe way:

$$n_d = \begin{cases} n_r & L \le d_0 \\ an_r & L/2 \le d_0 < L \\ bn_r & L/4 \le d_0 < L/2 \\ cn_r & d_0 < L/4 \end{cases} \tag{8}$$

where a, b, c are constant parameters; n_r is a constant shaft speed; d_0 represents the distance between the ship and the center of the docking area.

D. COLLISION AVOIDANCE MECHANISM

This section proposes a concept of risk factor representing the degree of danger for ship collision avoidance. It takes the ship's maneuvering characteristics, ship domain and relative speed between encountered ships into account. Based on the risk factor, evasive actions complying with rule 13-15 in COLREGs can be generated.

1) SHIP's MAXIMUM ADVANCE

Inspired by [28], ship's maneuvering characteristics should be considered when designing the collision avoidance mechanism. A maneuvering characteristic can be evaluated by changing or keeping a predefined course and speed of the ship. In this study, we apply the turning circle approach to evaluate how well the steering machine performs under course-changing maneuvers [25], [29].

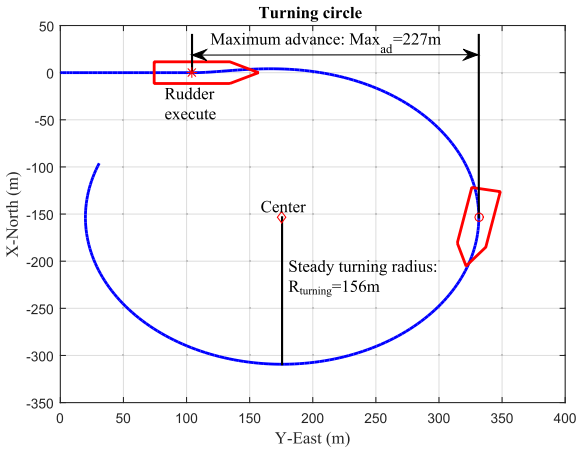

FIGURE 5. Turning circle maneuver using a constant rudder angle ($\delta = -15°$) at $t = 150s$.

Turning circle is generally used to obtain a ship's maximum advance and steady turning radius. Fig. 5 shows an example of the turning circle maneuver using the test ship from Section IV. The ship sails forward from still with a zero rudder angle. A constant rudder angle ($\delta = -15°$) is applied at $t = 150\,s$, resulting in a maximum advance of $Max_{ad} = 227m$ and a steady turning with a radius $R_{turning} = 156\,m$. We apply Max_{ad} to ship bumper construction. For details, please refer to Section III-D2.

2) SHIP BUMPER CONSTRUCTION

This section introduces how to build a ship bumper for collision avoidance. An ship bumper is an expansion of ship domain, which servers as a decision maker for switching between "path following" and "collision avoidance" in this study.

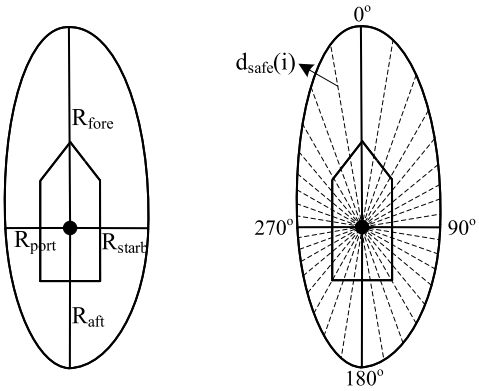

(a) Quaternion ship domain (b) Ship domain division

FIGURE 6. Wang's ship domain model and its division for ship bumper construction.

The concept of ship domain has been widely applied to marine traffic engineering for years [30], [31]. Here, we adopt Wang's method for ship domain construction [32]. This method is reliable and flexible since it takes manoeuvring

capability, speeds and courses into account. Fig. 6(a) is the schematic diagram of the domain. The ship domain consists of four quarter ellipses determined by the following four radii:

$$\begin{aligned} R_{fore} &= (1 + 1.34\sqrt{k_{ad}^2 + (k_{dt}/2)^2})L \\ R_{aft} &= (1 + 0.67\sqrt{k_{ad}^2 + (k_{dt}/2)^2})L \\ R_{starb} &= (0.2 + k_{dt})L \\ R_{port} &= (0.2 + 0.75k_{dt})L \end{aligned} \tag{9}$$

where L is ship length; k_{ad} and k_{dt} represent gains and can be calculated as follows [32]:

$$\begin{aligned} k_{ad} &= 10^{0.3591lgU+0.0952} \\ k_{dt} &= 10^{0.5441lgU-0.0795} \\ U &= \sqrt{(u^2 + v^2)} \end{aligned} \tag{10}$$

where u and v stand for the surge speed and the sway speed of the ship, respectively.

Once the ship domain is built, we divide it into 36 parts, as shown in Fig. 6(b). The purpose is to obtain a vector of distances d_{safe} from center of the ship to the outline of the ship domain. A ship bumper can thus be obtained by incorporating the maximum advance from Section III-D1 into the distance vector:

$$d = d_{safe}(i) + Max_{ad} \qquad i \in \{1, 2, ...36\} \tag{11}$$

As the ship's turning capability is considered, the ship bumper can ensure there are enough space and time for the own ship to take actions and keep the ship domain free.

3) COLLISION RISK FACTOR AND CORRESPONDING ACTIONS

According to Fig. 2 (a), ship encounter type can be identified based on the relative direction and the position between the own ship and the target ship. For the port-crossing situation, a risk factor is designed as $f_{risk} = 0$, which can make the own ship act as a stand-on vessel to keep its course and speed; whereas for other encounter situations, considering both distance and velocity are important for collision avoidance, we design the risk factor by combing the ship bumper with the relative velocity in encounter:

$$f_{risk} = f_1(d_t) \times f_2(V_{relative}) \tag{12}$$

where $f_1(\cdot)$ and $f_2(\cdot)$ are functions of distance d_t and relative velocity $V_{relative}$ between the own ship and the target ship, respectively. The first part of the risk factor $f_1(d_t)$ can be computed by:

$$f_1(d_t) = \begin{cases} 1 - \frac{d_t}{d}, & d_t < d \\ 0, & d_t \geq d \end{cases} \tag{13}$$

where d_t is the distance between the own ship and the target ship; d is the ship bumper distance. The second part of the risk factor $f_2(V_{relative})$ is defined as:

$$f_2(V_{relative}) = tanh(V_{relative}) \tag{14}$$

According to the risk factor, the desired heading angle ψ_d and thruster shaft speed n_d are set as follow:

$$\psi_d = \psi_0 + g(f_{risk}) \tag{15}$$

$$n_d = n_0 + h(f_{risk}) \tag{16}$$

where ψ_0 and n_0 represent the heading angle and thruster shaft speed at the moment when the ship entering "collision avoidance" mode, respectively; $g(f_{risk})$ and $h(f_{risk})$ are the compensation functions of heading angle and thruster shaft speed, respectively (The implementation please refer to Section IV). The desired ψ_d and n_d are further converted into control commands to the own ship by using a PID controller and a linear function, respectively:

$$\begin{aligned} n_c &= purelin(n_d) \\ \delta_c &= k_p(\psi - \psi_d) + k_i \int (\psi - \psi_d)dt + k_d r \end{aligned} \tag{17}$$

where n_c and δ_c stand for commands of thruster shaft speed and rudder angle; k_p, k_i and k_d are coefficients of the PID controller, respectively.

From (12)-(14), it is evident that $f_{risk} > 0$ corresponds to the condition that an invasion of the ship bumper occurs. Therefore, we conclude the risk factor plays the same role as the ship bumper in switching between "path following" and "collision avoidance". Furthermore, Eq. (15) and (16) indicate different f_{risk} could generate different collision evasive maneuvers, depending on the implementation of the compensation functions $g(\cdot)$ and $h(\cdot)$. In principle, these compensation functions should be designed to ensure that higher value of f_{risk} results in more rapid evasive behaviour of the vessel. The total evasion time depends on f_{risk}. Only when f_{risk} reduces to zero will the ship stop "collision avoidance" and switch to "path following".

IV. EXPERIMENT

In this section, a number of numerical simulations are carried out to validate the proposed strategy. In order to reduce the fluctuations of commands for rudder angle and thruster shaft speed, fuzzy theory is employed to design $g(\cdot)$ and $h(\cdot)$:

$$g(f_{risk}) = \begin{cases} 0^\circ & 0.0 = f_{risk} \\ 10^\circ & 0.0 < f_{risk} \leq 0.2 \\ 20^\circ & 0.2 < f_{risk} \leq 0.4 \\ 40^\circ & 0.4 < f_{risk} \leq 0.6 \\ 60^\circ & 0.6 < f_{risk} \leq 0.8 \\ 90^\circ & 0.8 < f_{risk} \end{cases} \tag{18}$$

$$h(f_{risk}) = -f_{risk} \times n_0 \tag{19}$$

Table 3 lists the own ship's initial and final states. The slope of the virtual straight line is $k = 0.48$. Some constant parameters are defined as follow: $L = 93\ m$, $A_F = 400\ m^2$, $A_L = 950\ m^2$, $\rho_a = 1.224\ kg/m^3$, and $n_r = 200\ rpm$. The simulation time step is set to $1\ s$. The PID controller are set to $k_p = 20$, $k_i = 0$, $k_d = 2$. Besides, the parameters in Eq. (8) are set to $a = 0.75$, $b = 0.5$, and $c = 0$. In addition, dynamic wind influence is considered in the experiment.

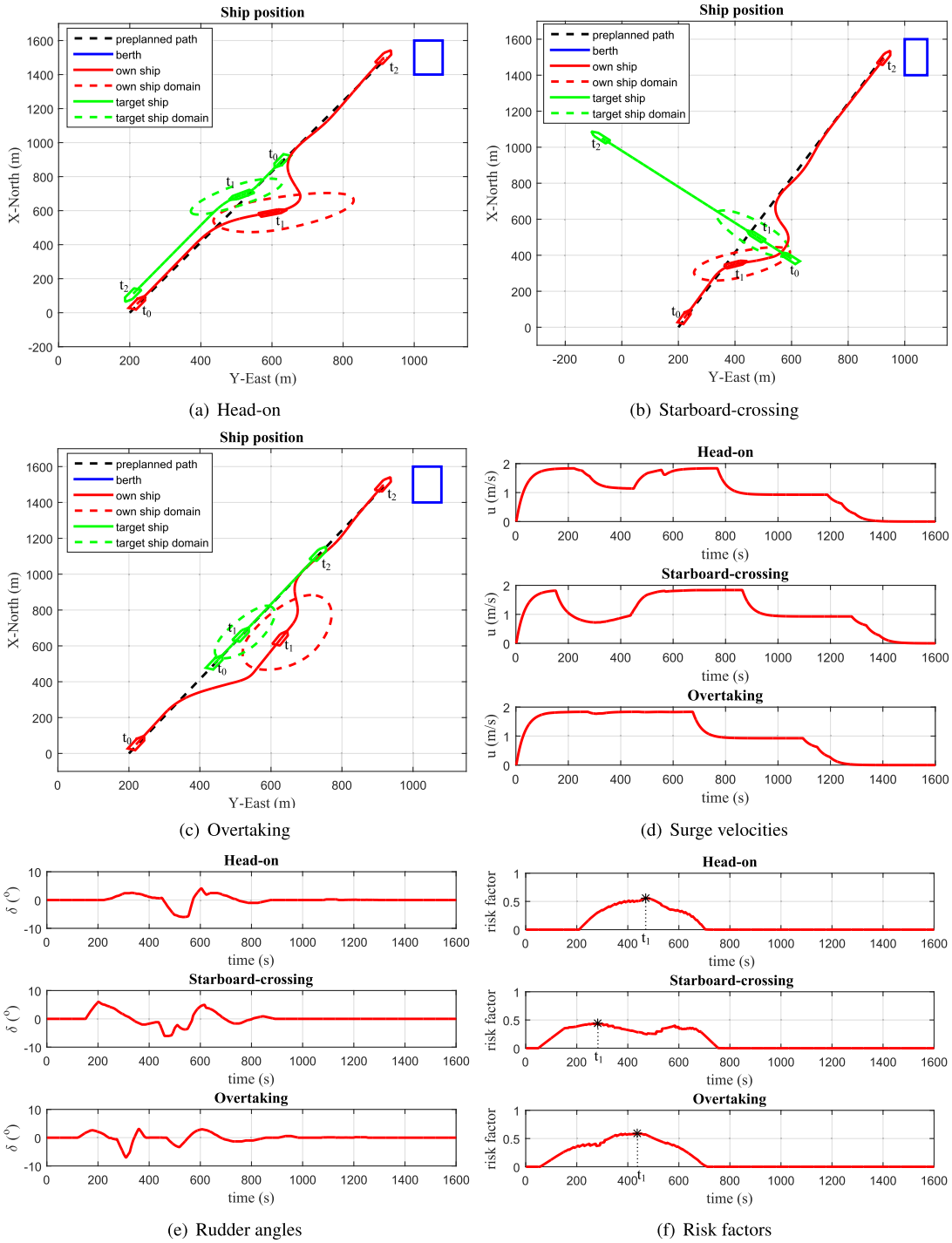

FIGURE 7. Ship maneuvering toward the dock without wind influence.

TABLE 3. Initial and final states of the own ship.

	$x(m)$	$y(m)$	$\psi(^o)$	$u(m/s)$	$v(m/s)$	$r(rad/s)$
Initial state	50	230	22	0	0	0
Final state	1500	900	25	0	0	0

A. SHIP MANEUVERING WITHOUT WIND INFLUENCE

The proposed control strategy is verified under three encounter situations: head-on, starboard-crossing and overtaking, without any wind influence. In the head-on case, each ship sails in an opposite direction along the pre-planned path at a different constant speed. Fig. 7 (a) shows the numerical result. It contains the whole maneuvering process from the start time t_0 when the own ship following the planned path to the final time t_2 when it approaches the vicinity of the berth. Both ships have made appropriate actions according to the rules in COLREGs to achieve port-to-port passing maneuver with a max risk factor $f_{risk} = 0.57$ (corresponding to the

situation at time t_1). The surge speed and the rudder angle of the own ship are shown in the top panel of Fig. 7 (d) and Fig. 7 (e), respectively. The results indicate that the own ship simultaneously adjusts its shaft speed and rudder angle to avoid collision with the target ship from approximately 200 s to 800 s. Here we omit the sway speed and the yaw rate since they are always in a range close to zero, i.e., $|v| < 0.23\ m/s$ and $|r| < 0.022\ rad/s$, respectively (They are also ignored in the rest of the experiment due to the slight effect on maneuvering.). The top panel of Fig. 7 (f) depicts the changes of the risk factor. It increases from 200 s to the peak 0.57, and gradually decreases to zero in the following 300 seconds.

Simulation with single obstacle starboard-crossing case is shown in Fig. 7 (b), from the start time t_0 until the own ship reaches the dock at time t_2. In this case, the target ship acts as a stand-on ship. The own ship takes starboard-crossing action as a give-way ship to avoid collision by adjusting its rudder angle and thruster shaft speed. The middle panel of Fig. 7 (d) and (e) show that the own ship reduces its surge speed by half and alters its rudder angle accordingly, resulting in a smooth turning to the right. The middle panel of Fig. 7 (f) illustrates how the risk factor changes over time. The peak value $f_{risk} = 0.48$ corresponds to the situation at time t_1 in Fig. 7 (b).

Fig. 7 (c) is the numerical result for the overtaking case. The target ship is a stand-on ship this time. The own ship changes its course in a good time and passes the target ship on the starboard side. After that, it steers back to the imaginary line until it approaches the dock. The corresponding surge velocity and rudder angle in Fig. 7 (d) and (e) show that the own ship keeps its speed during the overtaking process; only alters the rudder angle accordingly to achieve the overtaking. The corresponding risk factor, as shown in the bottom panel of Fig. 7 (f), increases as the own ship gets closer to the target ship, reaches the peak $f_{risk} = 0.62$ at time t_1, and decreases to zero after the overtaking is complete.

B. SHIP MANEUVERING UNDER WIND INFLUENCE

There are mainly two challenges in the maneuvering process: one is the interference with the target ships; the another is environmental effects, especially the effect from the wind. Here, we add dynamic wind disturbance to further verify the effectiveness of the proposed control strategy. The wind speed is set $V_w = 6\ m/s$, and its direction β_w is changed randomly during the maneuvering. Considering the wind direction cannot change dramatically in a short period of time, we assume that it changes every 100 seconds within a range of $[-20°, 20°]$, as depicted in Fig. 8.

Fig. 9 (a) illustrates the simulation results for the head-on case. Initially, the own ship follows the imaginary line, whereas the target ship sails from the opposite direction at time t_0. Then the two ships switch to ''collision avoidance'' mode when their risk factor values become greater than zero. By adjusting the rudder angle and thruster shaft speed, each ship succeeds to pass from the port side of the other ship

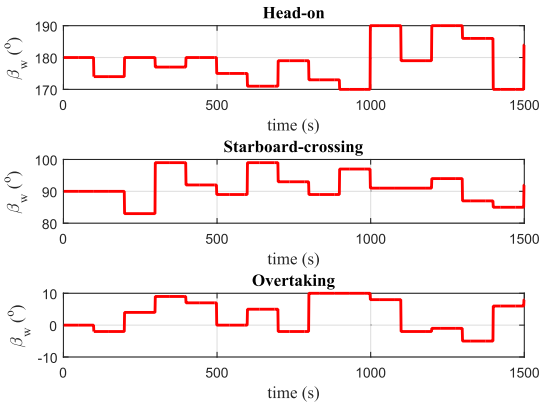

FIGURE 8. Randomly generated wind direction in the three encounter situations.

(see the situation at time t_1 for example). This is compliant with the main rules of COLREGs. After the risk factor falling back to zero, as shown in the top panel of Fig. 9 (f), the own ship enters the ''path following'' model again. Due to the wind perturbation, it cannot completely follow the imaginary line. Nevertheless, the own ship manages to reach the docking area at time t_2.

The experimental result for single obstacle starboard-crossing situation under dynamic wind disturbance is shown in Fig. 9 (b). It is noted that the result is similar to that of the crossing case without wind influence: the own ship makes a detour from the aft side of the target ship with the maximum risk factor $f_{risk} = 0.51$. In addition, there are also similarities in terms of surge speed, rudder angle, and risk factor, as shown in the middle panels of Fig. 9 (e)-(f). But compared to the total maneuver time of the starboard-crossing case in Section IV-A, the maneuver takes about 100 seconds more to complete the task, due to wind perturbation.

Fig. 9 (c) illustrates the result of the overtaking case under wind effect. Again, the trajectory of the own ship is similar to the trajectory of the corresponding case in Fig. 7 (c). The trend of surge speed, rudder angle, risk factor, and even the total maneuver time, as shown in the bottom panels of Fig. 9 (d), (e) and (f) are close to those in the corresponding panels of Fig. 7 (d)-(f).

There are also some differences compared to the overtaking case in Section IV-A. For example, the target ship is off the course slightly due to the wind effect, which results in a higher peak of risk factor $f_{risk} = 0.68$ during the maneuver. Furthermore, both the surge speed and the rudder angle of the own ship are non-zero when the ship reaches the dock, which indicates an inferior performance compared to the corresponding case in Section IV-A. The main reason is that the wind, especially the lateral wind, has a great influence on ship course.

C. EFFECT OF RISK FACTOR

In order to verify the effect of the risk factor, here we compare two strategies: the first one is the proposed strategy; the

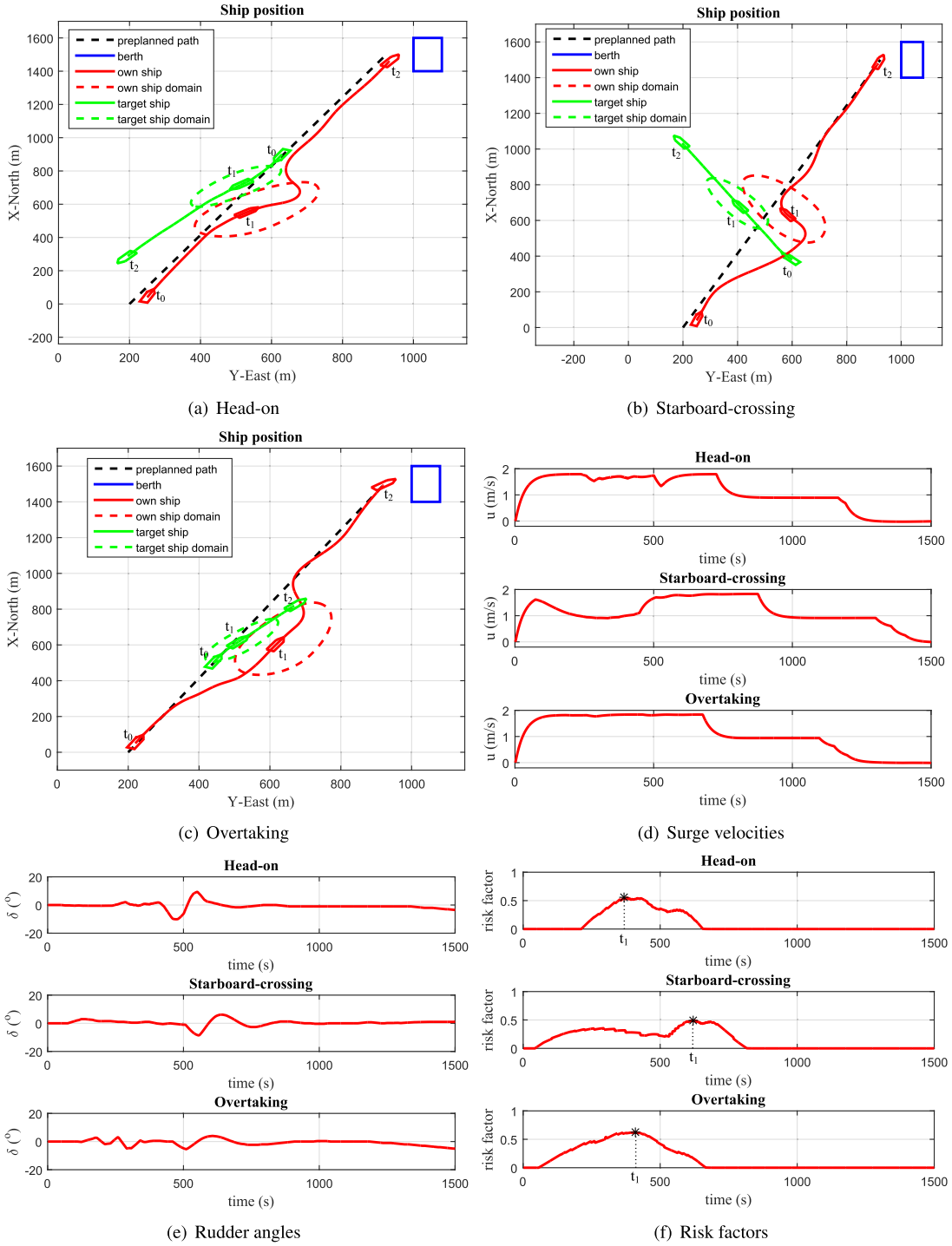

FIGURE 9. Ship maneuvering toward the dock under wind influence.

another one is a simplified strategy that it does not use the risk factor but steers the ship to the right directly when any target ships invade the ship bumper of the own ship (i.e., the variable d in Eq. (11).

Fig. 10 (a), (b) and (c) depicts the ships' trajectories using the two strategies in three different encounter situations. It is noted that the trajectory from the proposed method is smoother and closer to the planned imaginary path in each situation; the corresponding path length is shorter than that of the simplified strategy, as illustrated in the third column of Table 4. Furthermore, from the last three columns of Table 4, although a relatively longer computation time for the proposed method is needed in each encounter case, the curvature of the trajectory generated by the proposed

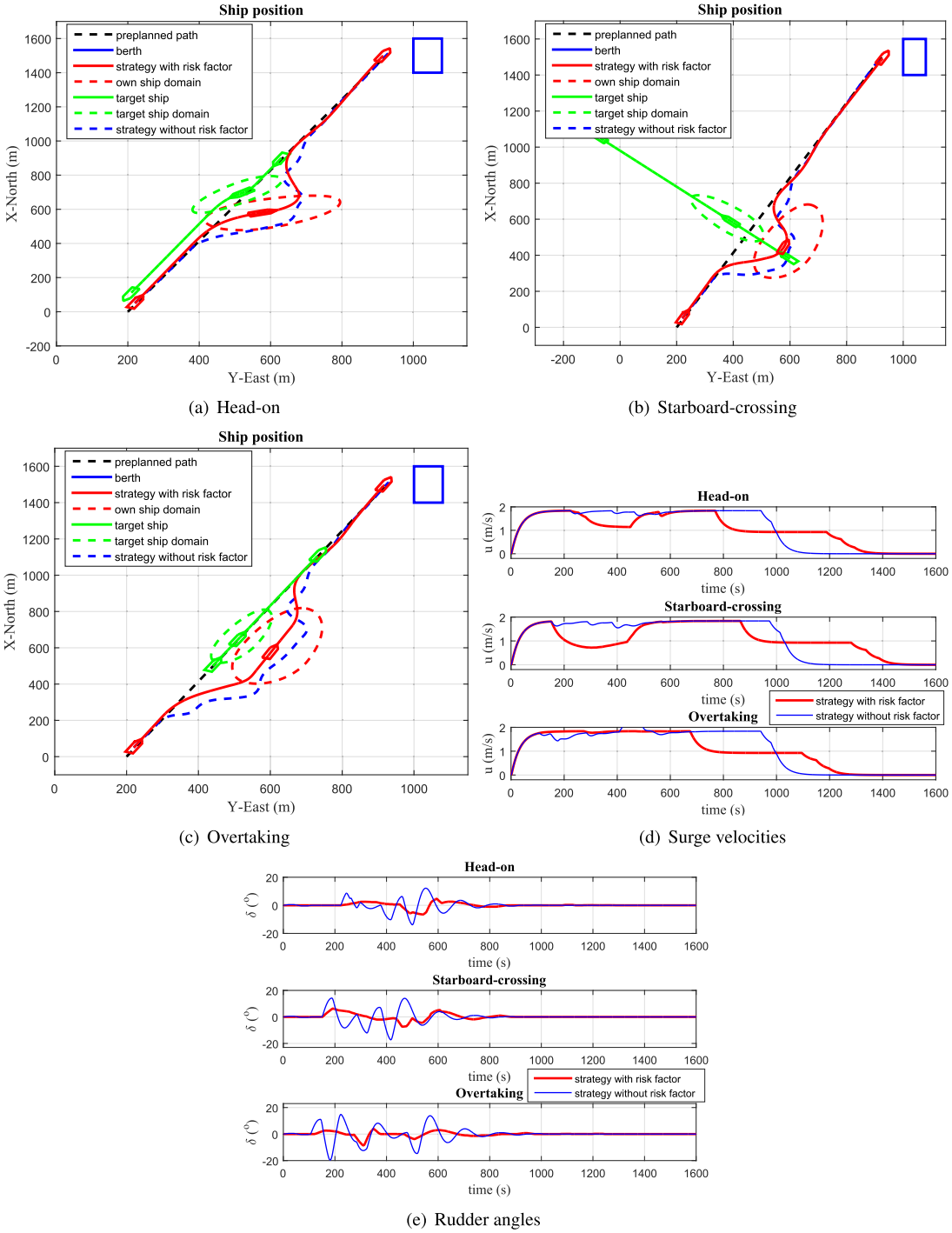

FIGURE 10. **Comparison of two strategies with and without risk factor.**

method is smaller than that of the simplified strategy. This implies the proposed strategy takes more about ship stability into consideration. In Fig. 10 (d), it is worth noting that the proposed strategy slows down the own ship when taking anti-collision actions; whereas the other strategy keeps the sailing speed, resulting in a shorter maneuver time to the dock. The changes of rudder angles from Fig. 10 (e) reveal that the rudder angle by the simplified strategy is more prone to fluctuations, especially when encounters occur. From the above comparison, it is evident to see that the risk factor plays a key role in generating anti-collision actions.

TABLE 4. Comparison with the strategy without risk factor.

Encounter situations	Methods	Total path length (m)	Distance between the ship and the imaginary line (m)		Curvature		Computation time(s)
			Max	$Average$	Max	$Average$	
Head-on	Proposed strategy	1.6924×10^3	143.8084	13.3121	0.0218	0.0017	249.54
	Simplified strategy	1.7453×10^3	177.7291	24.4897	0.3578	0.0033	212.84
Crossing	Proposed strategy	1.7100×10^3	147.6631	22.1808	0.0158	0.0019	261.65
	Simplified strategy	1.7912×10^3	189.7504	25.9333	0.0197	0.0038	231.02
Overtaking	Proposed strategy	1.6595×10^3	120.4155	20.0071	0.0195	0.0015	253.13
	Simplified strategy	1.7574×10^3	170.2722	33.9198	0.2283	0.0041	217.24

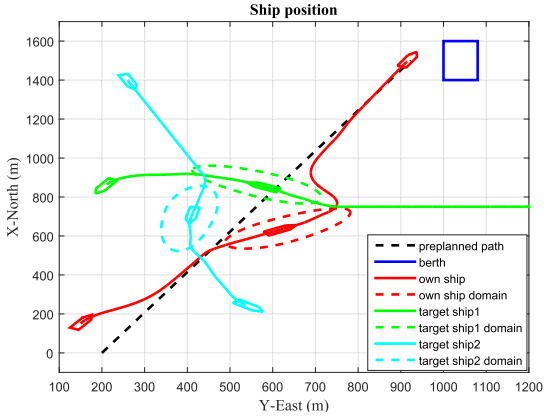

(a) Ship paths

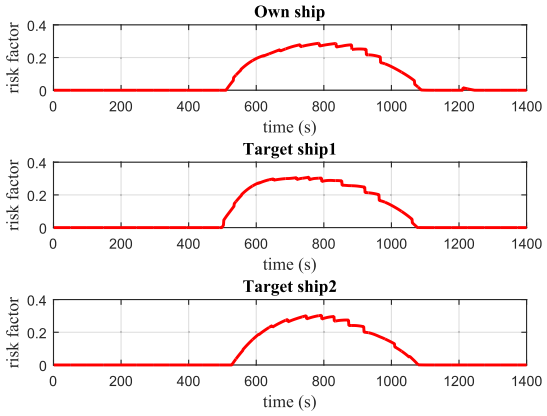

(b) Risk factors for the three ships

FIGURE 11. Ship maneuvering toward the dock under multi-ship encounter situation.

D. DISCUSSION

The experimental results show that the own ship can not only avoid the obstacle ships safely, but also reach the docking area accurately according to the commands from the proposed control strategy. In fact, the proposed strategy can also deal with port-crossing encounter. In such a situation, the own ship will act as a stand-on vessel and keep its course and speed. Of course, the strategy inevitably has some shortcomings. For example, the strategy is designed to generate path with small curvature, not only taking into account ship stability, but also avoiding saturation of rudder angle. This may result in slow alteration of ship course. Nevertheless, the bumper distance from Eq. (11) guarantees that the own ship can take action in good time. An example is the head-on encounter in Fig. 7. Although there is a deceleration from about $t \approx 300\ s$ caused by Eq. (15) and (19), the advance distance introduced to the collision avoidance mechanism enables the own ship to react as early as the target ship enters the bumper area. Therefore, even though the own ship decelerates slightly for the head-on situation in Fig. 7, it makes a clear course alteration that is readily apparent to the target ship. Another deficiency is that the control results under dynamic wind condition are not as good as these under no wind condition. The main reason may be that the low-speed maneuver when the ship is close to the dock reduces its maneuverability; the wind disturbance in such a situation can result in an inferior maneuvering performance.

Although this paper mainly focuses on the maneuvering strategy with single encounter, it is possible to extent the strategy to deal with more complicated scenarios, e.g., to interact with multiple COLREGs-compliant target ships. Here we give an example of ship maneuvering toward a dock under multi-ship crossing encounter situation. Assume there are two target ships coming across the own ship who is approaching the dock, as shown Fig. 11 (a). Each ship acts as a give-way vessel and keeps outside of the ship domain of other ships. The result shows the three ships take actions that are compliant with COLREGs. After the evasive maneuver, the own ship is steered back to the planned path and reaches the port successfully. Fig. 11 (b) illustrates that the three ships have a similar trend of risk factor. It reveals that if the control strategy is applied to all the involved ships, the values of the risk factor will be distributed equally to each ship, to minimize the risk of the whole encounter system.

V. CONCLUSION

In this paper, an effective ship control strategy for collision-free maneuver toward a dock is proposed. Considering the challenges in the maneuvering problem, we not only integrate the LOS and PID methods, but also make necessary improvements for these specific encounter situations, such as integrating the maximum advance, constructing the ship bumper and designing the fuzzy control rules. More specifically, the strategy consists of a path following method and a collision avoidance mechanism. The path following method is developed to steer the ship along a planned docking path by using the LOS algorithm. A risk factor is designed for

the collision avoidance mechanism. It servers as a decision maker that help the ship to take actions complying with rules 13-15 of COLREGs. The ship can either follows the planned path or performs anti-collision maneuver, depending on whether a defined ship bumper has been invaded. Through numerical simulation, the proposed strategy is verified effective in sailing the ship to the dock in various encounters under wind disturbance.

Based on the current work and the discussion from Section IV-D, future work will focus on: (1) combining the ''path following'' mode and the ''collision avoidance'' mechanism in an efficient way to compensate more types of environmental effects, such as wave and current; (2) refining the collision avoidance mechanism to improve the speed control of the ship and make the corresponding evasive behavior be compliant with most rules in COLREGs; and (3) evaluating the work in waterway scenarios containing both static and dynamic obstacles in a professional maritime transportation simulator.

REFERENCES

[1] *Convention on the International Regulations for Preventing Collisions at Sea (COLREGs)*, Int. Maritime Org. (IMO), London, U.K., 1972.

[2] C. Edwards and S. Spurgeon, *Sliding Mode Control: Theory and Applications*. Boca Raton, FL, USA: CRC Press, 1998.

[3] N. Mizuno and S. Matsumoto, ''Design and evaluation of simple ship's automatic maneuvering system using sliding mode controller,'' *IFAC Proc. Volumes*, vol. 46, no. 33, pp. 67–72, 2013.

[4] N. Mizuno, N. Saka, and T. Katayama, ''A ship's automatic maneuvering system using optimal preview sliding mode controller with adaptation mechanism,'' *IFAC-PapersOnLine*, vol. 49, no. 23, pp. 576–581, 2016.

[5] L. Yuan and H.-S. Wu, ''Terminal sliding mode fuzzy control based on multiple sliding surfaces for nonlinear ship autopilot systems,'' *J. Mar. Sci. Appl.*, vol. 9, no. 4, pp. 425–430, Dec. 2010.

[6] A. Maki, N. Sakamoto, Y. Akimoto, H. Nishikawa, and N. Umeda, ''Application of optimal control theory based on the evolution strategy (CMA-ES) to automatic berthing,'' *J. Mar. Sci. Technol.*, vol. 25, no. 1, pp. 221–233, 2019.

[7] N. Mizuno, Y. Mitake, T. Okazaki, and K. Ohtsu, ''A ship's minimum time maneuvering system with neural network and non-linear model based super real-time simulator,'' in *Proc. Eur. Control Conf. (ECC)*, Sep. 2003, pp. 1978–1983.

[8] N. Mizuno, H. Kakami, and T. Okazaki, ''Parallel simulation based predictive control scheme with application to approaching control for automatic berthing,'' *IFAC Proc. Volumes*, vol. 45, no. 27, pp. 19–24, 2012.

[9] N. Mizuno, Y. Uchida, and T. Okazaki, ''Quasi real-time optimal control scheme for automatic berthing,'' *IFAC-PapersOnLine*, vol. 48, no. 16, pp. 305–312, 2015.

[10] H. Yamato, ''Automatic berthing by the neural controller,'' in *Proc. 9th Ship Control Syst. Symp.*, vol. 3, 1990, pp. 3183–3201.

[11] N. Im and K. Hasegawa, ''A study on automatic ship berthing using parallel neural controller,'' *J. Kansai Soc. Nav. Architects, Jpn.*, vol. 2001, no. 236, pp. 65–70, 2001.

[12] P.-H. Nguyen and Y.-C. Jung, ''Automatic berthing control of ship using adaptive neural networks,'' *J. Navigat. Port Res.*, vol. 31, no. 7, pp. 563–568, Sep. 2007.

[13] Y. A. Ahmed and K. Hasegawa, ''Automatic ship berthing using artificial neural network based on virtual window concept in wind condition,'' *IFAC Proc. Volumes*, vol. 45, no. 24, pp. 286–291, Sep. 2012.

[14] Y. A. Ahmed and K. Hasegawa, ''Automatic ship berthing using artificial neural network trained by consistent teaching data using nonlinear programming method,'' *Eng. Appl. Artif. Intell.*, vol. 26, no. 10, pp. 2287–2304, Nov. 2013.

[15] Y. Shuai, G. Li, X. Cheng, R. Skulstad, J. Xu, H. Liu, and H. Zhang, ''An efficient neural-network based approach to automatic ship docking,'' *Ocean Eng.*, vol. 191, Nov. 2019, Art. no. 106514.

[16] N.-K. Im and V.-S. Nguyen, ''Artificial neural network controller for automatic ship berthing using head-up coordinate system,'' *Int. J. Nav. Archit. Ocean Eng.*, vol. 10, no. 3, pp. 235–249, May 2018.

[17] V.-S. Nguyen, V.-C. Do, and N.-K. Im, ''Development of automatic ship berthing system using artificial neural network and distance measurement system,'' *Int. J. FUZZY Log. Intell. Syst.*, vol. 18, no. 1, pp. 41–49, Mar. 2018.

[18] T. Statheros, G. Howells, and K. M. Maier, ''Autonomous ship collision avoidance navigation concepts, technologies and techniques,'' *J. Navigat.*, vol. 61, no. 1, pp. 129–142, Jan. 2008.

[19] C. Tam, R. Bucknall, and A. Greig, ''Review of collision avoidance and path planning methods for ships in close range encounters,'' *J. Navigat.*, vol. 62, no. 3, pp. 455–476, Jul. 2009.

[20] H. Shen, H. Hashimoto, A. Matsuda, Y. Taniguchi, D. Terada, and C. Guo, ''Automatic collision avoidance of multiple ships based on deep *Q*-learning,'' *Appl. Ocean Res.*, vol. 86, pp. 268–288, May 2019.

[21] T. A. Johansen, T. Perez, and A. Cristofaro, ''Ship collision avoidance and COLREGS compliance using simulation-based control behavior selection with predictive hazard assessment,'' *IEEE Trans. Intell. Transp. Syst.*, vol. 17, no. 12, pp. 3407–3422, Dec. 2016.

[22] M.-C. Lee, C.-Y. Nieh, H.-C. Kuo, and J.-C. Huang, ''A collision avoidance method for multi-ship encounter situations,'' *J. Mar. Sci. Technol.*, vol. 2019, pp. 1–18, Nov. 2019.

[23] C. Tam and R. Bucknall, ''Collision risk assessment for ships,'' *J. Mar. Sci. Technol.*, vol. 15, no. 3, pp. 257–270, Sep. 2010.

[24] L. Zhao and M.-I. Roh, ''COLREGs-compliant multiship collision avoidance based on deep reinforcement learning,'' *Ocean Eng.*, vol. 191, Nov. 2019, Art. no. 106436. [Online]. Available: http://www.sciencedirect.com/science/article/pii/S0029801819305840

[25] T. I. Fossen, *Handbook of Marine Craft Hydrodynamics and Motion Control*. Hoboken, NJ, USA: Wiley, 2011.

[26] K.-P. Lindegaard, ''Acceleration feedback in dynamic positioning,'' Ph.D. dissertation, Dept. Eng. Cybern., Norwegian Univ. Sci. Technol., Trondheim, Norway, 2003.

[27] T. Fujiwara, M. Ueno, and T. Nimura, ''Estimation of wind forces and moments acting on ships,'' *J. Soc. Nav. Architects Jpn.*, vol. 1998, no. 183, pp. 77–90, 1998.

[28] R. Szlapczynski and J. Szlapczynska, ''An analysis of domain-based ship collision risk parameters,'' *Ocean Eng.*, vol. 126, pp. 47–56, Nov. 2016.

[29] M. Reichel, ''Application of the IMO standard manoeuvres procedure for pod-driven ships,'' *J. Mar. Sci. Technol.*, vol. 25, pp. 249–257, May 2019.

[30] Y. Fujii and K. Tanaka, ''Traffic capacity,'' *J. Navigat.*, vol. 24, no. 4, pp. 543–552, 1971.

[31] W. Zhang, F. Goerlandt, P. Kujala, and Y. Wang, ''An advanced method for detecting possible near miss ship collisions from AIS data,'' *Ocean Eng.*, vol. 124, pp. 141–156, Sep. 2016.

[32] N. Wang, ''An intelligent spatial collision risk based on the quaternion ship domain,'' *J. Navigat.*, vol. 63, no. 4, pp. 733–749, Oct. 2010.

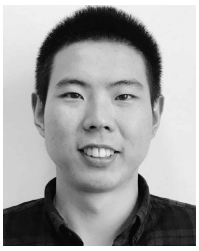

YONGHUI SHUAI is currently pursuing the master's degree with the Zhejiang University of Technology, Hangzhou, China, in 2017. In 2018, he visited the Department of Ocean Operations and Civil Engineering, Norwegian University of Science and Technology, Aalesund, Norway, for exchange study. His current research interests include automatic control, neural networks, and ship motion modeling.

GUOYUAN LI (Senior Member, IEEE) received the Ph.D. degree from the Department of Informatics, Institute of Technical Aspects of Multimodal Systems (TAMS), University of Hamburg, Hamburg, Germany, in 2013. In 2014, he joined the Mechatronics Laboratory, Department of Ocean Operations and Civil Engineering, Norwegian University of Science and Technology, Norway. In 2018, he was an Associate Professor in ship intelligence. He has published over 50 articles in these areas. His research interests include eye tracking analysis, modeling and simulation of ship motion, artificial intelligence, optimization algorithms, and locomotion control of bio inspired robots.

JINSHAN XU (Member, IEEE) received the Ph.D. degree in physics from the École Normale Supérieure de Lyon, in 2013. He is currently a Lecturer with the College of Computer Science and Technology, Zhejiang University of Technology. His research interests include organic tissue modeling, signal processing, and automatic control.

HOUXIANG ZHANG (Senior Member, IEEE) received the Ph.D. degree in mechanical and electronic engineering, in 2003, and the Habilitation degree in informatics from the University of Hamburg, in February 2011. In 2004, he was a Postdoctoral Fellow with the Department of Informatics, Faculty of Mathematics, Informatics and Natural Sciences, Institute of Technical Aspects of Multimodal Systems (TAMS), University of Hamburg, Germany. He joined the Norwegian University of Science and Technology, in April 2011, where he is currently a Professor in robotics and cybernetics. He has published over 130 journal and conference papers and book chapters as an author or coauthor in these areas. His research interests include two areas, such as biological robots and modular robotics and virtual prototyping and maritime mechatronics.